On the Self-assembly of Perfluoroalkylalkanes

Luís Belchior[‡,†], George Jackson[†], Eduardo Filipe[‡,*]

[‡]Instituto Superior Técnico, Avenida Rovisco Pais, 1, 1049-001 Lisbon, Portugal; [†]Imperial College, South Kensington Campus, SW7 2AZ London, United Kingdom

KEYWORDS Perfluoroalkylalkanes – Coarse-Grained – Molecular Dynamics – SAFT-γ Mie EoS

ABSTRACT: In this work, Molecular Dynamics (MD) simulations were used to study the interfacial behaviour and the self-assembly of mixtures of Perfluoroalkylalkanes (PFAAs) in hydro- and fluorocarbon solvents. PFAAs are linear di-block copolymers formed from an alkane and a perfluoroalkane chains bonded together, with the general formula $F(CF_2)_n(CH_2)_mH$ (shortened for F_nH_m). The distinct amphiphilic character imparted by these two mutually phobic chains (importantly named *primitive surfactants*) is known to contribute to promote supramolecular organization. A recently developed heteronuclear *coarse-grained* (CG) force field of the SAFT-γ Mie family was refined. A new set of fluorinated beads was defined and the intramolecular terms of the force field determined via Direct Boltzmann Inversion from United-Atom simulations. Additionally, the SAFT-γ Mie Equation of State was used to obtain the intermolecular Mie potentials between the novel CG groups from thermodynamic data. The theory accurately described bulk properties, as well as critical points, of perfluoroalkanes and PFAAs, even for compounds not included in the modelling procedure. Furthermore, supramolecular organization in the referred mixtures was detected, with the model – despite its simplicity – capturing the subtleties arising from the interactions between PFAAs and the solvent. In so doing, this work can be used to further refine the industrial practice of fluorinated compounds and provide the means to advance the understanding of aggregation of this important surfactant family.

1. Introduction

Perfluoroalkylalkanes (PFAAs) are linear copolymers comprising a perfluoroalkyl and an alkyl chains chemically bonded together, with the general formula $F(CF_2)_n(CH_2)_mH$ (shortened for F_nH_m) [1]. The non-ideality that characterizes the mixtures of perfluoroalkanes (PFAs) and alkanes (reflected on the large positive deviations to Raoult's Law, on the large positive excess volumes and on their liquid-liquid partial miscibility, etc.) confers PFAAs a marked amphiphilic character, as both segments of the copolymer nurture a mutual phobicity to each other [2]. What's more, because both perfluoroalkanes and alkanes are hydrophobic (and apolar), this amphiphilicity is not based on the usual hydrophilic/hydrophobic opposition, PFAAs have been called *primitive surfactants* [3] – and since this opposition is exclusively ruled by (weak) van der Waals' forces, the overall interactions landscape is very subtle one.

PFAAs have been reported: to aggregate in solvents chemically similar to one of their tails [4, 5]; to display surface freezing [6]; to positively interfere with the miscibility of fluoroalkane – alkane mixtures interface [7]; among many other features.

The scarcity of experimental data, namely interfacial data (which is of paramount importance to grasp the organization of PFAAs in the different circumstances described) has fuelled the development

of force fields to be applied in computer simulations. Earlier atomistic force fields such as OPLS [8] or TraPPE [9] gained widespread utilization when published, but were recently surpassed in accuracy and versatility by the UA model of Potoff *et al.* [10], which innovated by using the Mie, and not the Lennard-Jones, intermolecular potential (while keeping the OPLS part for the bonded interactions). However, the need to access larger time and length scales paved the way for the development of coarse-grained (CG) force fields, in which several heavy atoms (excluding Hydrogen) are gathered into one *superatom* or *bead*. In so doing, molecular simulations are necessarily fastened – not only are there less atoms (and thus less interactions to compute) but also the energy landscape is smoothed, preventing simulations from crashing as often as they do with more detailed models [11]. Recently, Morgado *et al.* [1] published a CG force field modelled with the Statistical Associating Fluid Theory (SAFT) that proved remarkably accurate in predicting bulk and interfacial properties of pure PFAAs. The present work aimed at further testing this force field in organization of mixtures of PFAAs in hydro- and fluorocarbon solvents.

This work starts with the identification of an important flaw on the previous CG model and its correction; it then proceeds to the reparameterisation of the force field and, in parallel, to the development of an intramolecular potential for the fluorocarbon chains. With a sound force field, prediction of bulk properties of pure components, as well as liquid-liquid equilibria (LLE) and vapour-liquid equilibria (VLE) of mixtures of alkanes and perfluoroalkanes, is undertaken. Then, with Molecular Dynamics simulations, surface tensions (ST) are estimated for pure PFAs and PFAAs; finally, systems of PFAAs in either hydro- or fluorocarbon solvents are simulated and its organization analyzed, with the influence of several parameters (such as temperature, solute concentration and fluorine content of the solute) on the surface tension systematized.

2. Molecular models and theoretical framework

2.1 Force field – intermolecular interactions

A force field is a mathematical expression that describes the interactions between particles. Presently, the intermolecular forces between CG beads in different molecules (or even CG beads in the same molecule, but more than 3 bonds from each other) are assumed to be well described through the Mie potential (Equation 1.1).

$$u_{MIE}(r) = C\varepsilon\left[\left(\frac{\sigma}{r}\right)^{\lambda_r} - \left(\frac{\sigma}{r}\right)^{\lambda_a}\right] \quad (1.1)$$

$$C(\lambda_a, \lambda_r) = \left(\frac{\lambda_r}{\lambda_r - \lambda_a}\right)\left(\frac{\lambda_r}{\lambda_a}\right)^{\frac{\lambda_a}{\lambda_r - \lambda_a}} \quad (1.2)$$

Equation 1.2 details the means to evaluate the pre-factor C so that the minimum of the Mie potential has a numerical value of -ε.

This model is more versatile than the Lennard-Jones and, in particular concerning perfluoroalkanes, the latter was demonstrated to be unsuited to accurately reproduce the vapour pressures and saturated liquid densities at the same time, let alone VLE of more complicated mixtures [10].

In light of Fritz London's theory of dispersion forces, the attractive exponent of the Mie potential, λ_a , was fixed at 6. The repulsive exponent was treated as another adjustable parameter, which was particularly relevant given the known stiffness and rigidity of the fluoroalkane chains.

This work had its theoretical foundations on SAFT-γ Mie, the latest "flavour" of SAFT, which describes chain molecules (such as PFAAs) as a sequence of heteronuclear segments, in which the interactions between the different atoms (or CG beads)

are described via a Mie potential. The SAFT-γ Mie framework provides a bridge between macroscopic properties and the intermolecular parameters (what is called a *top-down* procedure) [12].

2.2 Force field – intramolecular interactions

No matter how valuable SAFT may be for intermolecular forces, it is not used to grip intramolecular interactions, that is, to evaluate how rigid are the bonds between atoms; what is the angle between bonds; and what are the dihedral angles and the energy required to move between different conformations. In a research focused on aggregation, thus deeply related with the structure and the shape of molecules, these are critical concerns.

The intramolecular potential (often called the *bonded* potential, because it respects interactions between atoms in the same molecule, connected through chemical bonds) may be parameterised as in Equation 2. Note that both bond stretching and angle bending potentials follow a harmonic law.

$$U^{bonded}(r,\theta,\varphi) = \sum_{bonds} \frac{1}{2} k_{bond}(r - r_0)^2 + \sum_{angles} \frac{1}{2} k_{angle}(\theta - \theta_0)^2 + \sum_{dihedrals} \sum_{n=0}^{5} C_n \cos^n(\varphi) \quad (2)$$

where k_{bond} and k_{angle} are the stretching and bending constants, respectively; r_0 and θ_0 are the equilibrium bond length and angle, respectively; and C_n is the set of Ryckaert-Bellemans constants for the torsional term.

UA simulations were performed and Direct Boltzmann Inversion (DBI) [13] was used to obtain the parameters outlined above. This procedure is the same used before for alkanes [14], and it provides a reliable way to ensure that the structure of the CG molecule resembles the real one (or the atomistic one, which we take for accurate).

2.3 Set of beads – a critical analysis

The work of Morgado *et al.* [1], which precedes the present work, had a structural flaw that needed to be addressed: because the fluorinated beads were much smaller than the hydrogenated ones (1 or 2 carbon atoms vs. 3 or 4, respectively), the CG alkyl chain was paradoxically thicker than its fluorinated counterpart – against the molecular structure acknowledged to PFAAs. Fig. 1 portrays this imperfection.

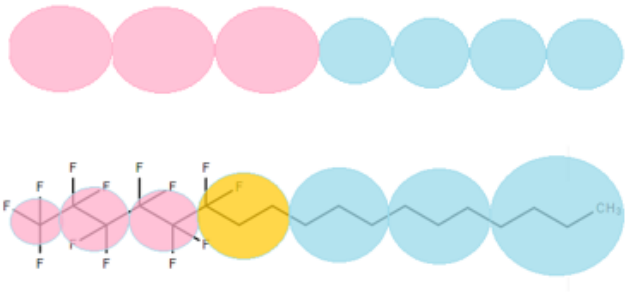

Figure 1 – "Natural" representation of a PFAA (above) and the twisted representation that the asymmetric mapping purveys (below). Circles colour scheme: pink stands for fluorinated beads; blue for hydrogenated beads; orange for the linker that connects both tails.

This skewed depiction convinced us to enlarge the fluorinated beads. On a first moment, the terminal bead was expanded from $–CF_3$ to $–CF_2–CF_3$; next, because keeping the fluorinated middle bead with two carbons would hinder the MD simulation of most of the PFAAs reported in the literature, this CG bead was also increased from $–CF_2–CF_3$ to $–CF_2–CF_2–CF_3$. Importantly, it was not possible, at this moment, to know whether or not this modification, though adding another layer of physical coherence to the structure purveyed by the CG model, would improve the overall performance of the model.

A helpful test that could be done immediately was to compute the radial distribution functions (RDFs) of both CG models and compare them with their UA counterparts – see Figs. 2 and 3.

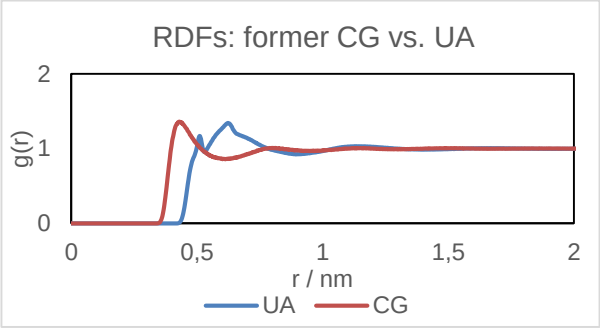

Figure 2 - Comparison of the RDF (evaluated between the centres of mass) of perfluorohexane at 373.15K and 5 bar, for both UA and CG models.

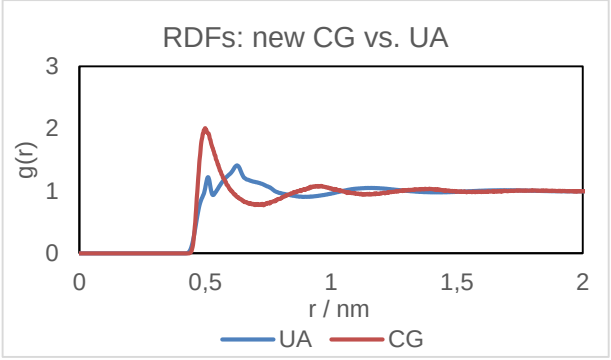

Figure 3 - Comparison of the RDF (evaluated between the centres of mass) of perfluoroheptane at 373.15K and 5 bar, for both UA and CG models.

By closing the gap that the former model had between the lift-off of the CG and the UA RDFs, the new set of beads is expected to better reproduce the real structure of the molecule. The new set of beads is resumed on Table 1. Notice that the alkane beads and the linker (group FH) were kept unchanged.

Table 1 - New set of beads.

Name	All-atom
FE	$CF_3 – CF_2 –$
FM	$– C_3F_6 –$
FH	$– CF_2C_2H_4 –$
CE	$C_3H_7 –$
CM	$– C_3H_6 –$
-C4	$C_4H_9 –$

Moreover, in [1], the intramolecular parameters for the PFAs were not determined – and the values for the alkanes, clearly not as stiff as PFAs, were used instead. By determining the set of parameters for the fluorocarbon chains, the model hereby proposed gained much more physical significance than the one published before.

3. Force field Development

3.1 Intermolecular parameters

Since PFAAs are the ultimate goal of this modelling, we divided the necessary parameters in three categories: those concerning exclusively perfluoroalkanes; the unlike interactions between hydrogenated and fluorinated beads; and, finally, the parameters for the linker (group FH in Table 1), which bridges both alkyl and perfluoroalkyl segments in a PFAA. We underline that the intermolecular parameters for the alkane beads were already determined in [14].

Among those referred above, there are the parameters characterizing each group but also *cross parameters*, which concern the interactions between two different groups. The cross interactions were, in this work, calculated with the Equations 3.1 (for size parameter), 3.2 (for the repulsive exponent) and 3.3 (for the energy parameter) [1, 12].

$$\sigma_{ij} = \frac{\sigma_{ii} + \sigma_{jj}}{2} \quad (3.1)$$

$$\lambda_{ij} - 3 = \sqrt{(\lambda_{ii} - 3)(\lambda_{jj} - 3)} \quad (3.2)$$

$$\varepsilon_{ij} = \left(1 - k_{ij}\right) \frac{\sqrt{\sigma_{ii}^3 \sigma_{jj}^3}}{\sigma_{ij}^3} \sqrt{\varepsilon_{ii}\varepsilon_{jj}} \quad (3.3)$$

In Equation 3.3, k_{ij} is an adjustable parameter meant to account to deviations to this modified-Berthelot rule. While the two first rules were always

used, the Berthelot-like rule is deemed to yield (in the absence of the k_{ij}) severe failures in predicting mixed properties [10, 15]. Therefore, two procedures were devised for cross intractions between similar groups (two fluorinated or two hydrogenated beads) and between dissimilar groups (a fluorinated and a hydrogenated one). For the former, k_{ij} was set to zero, since mixtures of alkanes with close lengths may be treated as ideal; for the latter, the cross ε_{ij} was regarded itself as an adjustable parameter and directly optimized with VLE data for mixtures of alkanes and perfluoroalkanes [16].

Table 2 - Successive steps undertaken during the sequential modelling, with the experimental data used in each step.

Step	Targeted Parameters	Experimental Data Used	Ref.
1.	FE: σ, λ_{rep}, ε FM: σ, λ_{rep}, ε	Saturated Liquid Densities and Vapour Pressures of F_4 and F_7 in the range $0.5T_c$ – $0.9T_c$	[17]
2.	FE – CM: ε FE – CE: ε FE – C4: ε FM – CM: ε FM – CE: ε FM – C4: ε	Vapour – Liquid Equilibria (composition of both phases) at constant temperature and pressure of: $F_5 + H_6$, $F_6 + H_5$, $F_6 + H_6$, $F_6 + H_7$, $F_6 + H_8$, $F_7 + H_6$, $F_8 + H_6$.	[16]
3.	FH: σ, λ_{rep}, ε FH – FE: ε FH – FM: ε FH – CE: ε FH – CM: ε FH – C4: ε	Saturated Liquid Densities and Vapour Pressures of F_4H_5, F_4H_6, F_4H_8, F_6H_6; Saturated Liquid Density of F_6H_8.	[18, 19]

As a "one-step" optimization – in which all experimental data was provided and all parameters were estimated – proved unsuccessful and physically meaningless, the estimation methodology encompassed three sequential steps. First, with bulk properties (vapour pressure and saturated liquid densities) of perlfuorobutane and perfluoroheptane, the like parameters for groups FE and FM were evaluated. Then, with VLE for alkane – PFA mixtures, the cross ε between HC and FC groups was optimized. Finally, with bulk properties for PFAAs (again, vapour pressure and saturated liquid densities), the like parameters for the linker were estimated, as well as the cross ε between the linker and all the other groups. Table 2 recaps the optimization procedure just described.

For steps 1 and 3, the objective function (to minimize) was given by Equation 4:

$$\min_{\alpha} F(\alpha) = \min_{\alpha} \sum_{i=1}^{N_\rho} \left(\frac{\rho_L(T_i, \alpha) - \rho_L^{exp}}{\rho_L^{exp}} \right)^2 + \sum_{k=1}^{N_P} \left(\frac{P_{vap}(T_k, \alpha) - P_{vap}^{exp}}{P_{vap}^{exp}} \right)^2 \quad (4)$$

while for step 2, the objective function was given, instead, by Equation 5:

$$\min_{\alpha} G(\alpha) = \min_{\alpha} \sum_{i=1}^{N_\rho} \left(\frac{y(T_i, P_i, x_i) - y^{exp}}{y^{exp}} \right)^2 \quad (5)$$

The optimization was carried on with the software gSAFT®, developed by the company Process System Enterprise (www.psenterprise.com). The final results are included on Tables 3 and 4.

Table 3 – Parameters for the like interactions. Recall that the like parameters for the alkanes (groups CM, CE and C4) were already published in [1].

Like Interactions				
MW (g/mol)	**Group**	**σ / Å**	**ε / K**	**λ_{rep}**
119.01	FE	4.637	322.14	25.29
150.02	FM	4.739	380.80	22.26
78.06	FH	4.533	330.09	17.11
42.08	CM	4.184	377.14	16.43
43.09	CE	4.501	358.37	15.95
57.11	C4	5.001	473.62	24.00

Table 4 – Parameters for the unlike interactions.

Unlike interactions				
		σ / Å	**ε / K**	**λ_{rep}**
FE	FM	4.688	350.18	23.72
	FH	4.585	393.13	20.73
	CM	4.410	349.26	20.30
	CE	4.569	322.03	19.99
	C4	4.819	348.52	24.64
FM	FH	4.636	302.86	19.49
	CM	4.461	355.34	19.08
	CE	4.620	341.12	18.79
	C4	4.870	420.74	23.11
FH	CM	4.358	283.30	16.77
	CE	4.517	331.81	16.52
	C4	4.767	397.72	20.21
CM	CE	4.343	366.90	16.19
	C4	4.593	417.63	19.79
CE	C4	4.751	410.27	19.49

3.2 Intramolecular parameters

Unlike the intermolecular interactions, which can be directly related to macroscopic properties, intramolecular forces required a bottom-up approach, in which more detailed simulations (UA) were performed. Through DBI, parameters for the harmonic laws for bond stretching and angle bending were obtained. Torsional barriers were neglected for they were always below $0.8k_BT$. Potoff's UA force field [10] was used.

As the fluorinated groups were $-C_2F_5$ (FE) and $-C_3F_6-$ (FM), the shortest PFAs that could be simulated were perfluoroheptane (F_7: FE-FM-FE) and perfluorodecane (F_{10}: FE-FM-FM-FE). Aiming at transferability and representability [20], simulations of both compounds were done at (373.15K, 5 bar) and (473.15K, 20 bar), in both the liquid and gas phase, with the final average taking into account all simulations. The final results are exhibited in Table 5.

Table 5 – Intramolecular parameters for CG simulations.

	Intramolecular parameters	
Bonds	r_0 / nm	σ
FE-FM	k_{bond} / kJ.mol^{-1}.Å^{-2}	630.94
Bonds	r_0 / nm	σ
FM-(FM,FH)	k_{bond} / kJ.mol^{-1}.Å^{-2}	514.85
Fluorinated Chains (comprising FE,FM,FH)	θ_0 / degrees	178.96
	k_{angle} / kJ.mol^{-1}.rad^{-2}	52.26
Bonds	r_0 / nm	σ
FH-(C4,CE,CM)	k_{bond} / kJ.mol^{-1}.Å^{-2}	61.30
Angles with FH and at least one (CM,CE,C4) group	θ_0 / degrees	159.90
	k_{angle} / kJ.mol^{-1}.rad^{-2}	17.66

4. Application of the Force Field

4.1 Bulk and Interfacial Properties Prediction

Once developed, the described force field was evaluated on the accuracy of its predictions. We started with bulk properties (saturated liquid density and vapour pressure) of perfluoroalkanes (F_4 to F_9) and perfluoroalkylalkanes (F_4H_5, F_4H_6, F_4H_8, F_6H_6, F_6H_8). The average of the average absolute deviations for each compound, as well as the associated standard deviation, are presented on Table 6. Due to scarcity of data, both F_5 and F_6H_8 were not accounted for on the vapour pressure calculation on Table 6.

The model is able to accurately predict, despite the coarse-graining (on average, 8 heavy atoms : 1 CG bead), the properties listed, namely for compounds not used in the modelling.

Table 6 - Average of AAD(%) and standard deviation for bulk properties prediction in PFAs and PFAAs.

	Vapour Pressure	Sat. Liq. Density
PFAs	0,89 ± 0,56 %	1,04 ± 0,46 %
PFAAs	1,97 ± 1,21 %	0,49 ± 0,20 %

The model was also able to accurately predict critical properties of perfluoroalkanes: an average deviation from experimental data [21] of 0,61% was achieved for the critical temperature (for F_4-F_9); roughly 4,16% for critical densities (for F_4-F_7); and approximately 8,13% for critical pressures (for F_4-F_7). The last results are less encouraging because of the exponential dependence of the vapour pressure with temperature, which worsens the performance of the model on this specific critical property.

VLE [16] and LLE [16, 22] of alkane – PFA mixtures were also tested, though with very different outcomes. At least partly because it was used in the modelling, agreement with experimental data for VLE was reasonably accurate (with deviations in the vapour phase composition averaging 2,77% for the mixtures listed on Table 3); for LLE, the model generally failed to predict UCSTs and critical compositions. The predictions were, nevertheless, much closer to experimental data when both alkane and perfluoroalkane had the same chain length; and the more different these lengths were, the larger the difference in the predicted UCSTs. Finally, surface tensions were estimated via the mechanical route, established in Equation 5.

$$\gamma = \frac{1}{2}\int_0^{L_z}\left(P_{zz} - \frac{1}{2}\left(P_{xx} + P_{yy}\right)\right)dz \approx \frac{L_z}{2}\left(\overline{P_{zz}} - \frac{1}{2}\left(\overline{P_{xx}} + \overline{P_{yy}}\right)\right) \quad (5)$$

The novel model proved accurate in the prediction of surface tensions of PFAs, PFAAs and *n*-dodecane. While the previous set of beads led to a slightly better agreement regarding PFAAs, the proposal followed in this paper achieved more exact outcomes concerning perfluoroalkanes. Deviations averaged below 0.5 mN/m for the latter (for F_7); around 1.70 mN/m for the former (for F_6H_6 and F_6H_8). For H_{12}, at 50ºC, simulations pointed out to an overestimation (26.40 mN/m vs. the experimental result of 22.70 mN/m). This is an important achievement since no interfacial property was used in the modelling; the referred agreement supports that this CG model captures the essential physical features of PFAAs.

4.2. Mixtures of PFAAs in solvents

Finally, the CG model was applied to mixtures of PFAAs in both hydro- and fluorocarbon solvents. PFAAs are prone to aggregate in solvents "*with a propensity for one of the chain segments*" [1]. The prepared simulations aimed to understand what are the differences arising from the presence of a fluorinated (F_7) or a hydrogenated (H_{12}) solvent; and what is the influence of several parameters in the organization of PFAAs, such as temperature, solute concentration and fluorine content of the solute.

For the sake of comparability (at least qualitatively), mixtures that had been tried experimentally were prepared for MD simulation. Based on [3], we started with $F_{12}H_{14}$ in H_{12} and F_9H_{15} in F_7.

4.2.1 PFAAs in *n*-dodecane

Let us consider a PFAA in dodecane (or any other alkane). On the one hand, given the mutual phobicity between perfluoroalkanes and alkanes, there is a driving force for the perfluoroalkanes to move towards the surface, so as to minimize the exposure to the solvent. On the other hand, because perfuoroalkanes have a consistently lower surface

tension than alkanes, the migration of the fluoroalkyl chains to the surface helps stabilizing the surface, thus decreasing the ST. Therefore, there is an overall driving force for the *positive adsorption* of PFAAs at the surface, with the fluorinated tails oriented outwards. This was confirmed by snapshots of $F_{12}H_{14}$ in H_{12}, at 1%mol and 4%mol (see Fig. 4). Positive adsorption is seen, with the fluorinated chains migrating towards the surface and emptying the bulk.

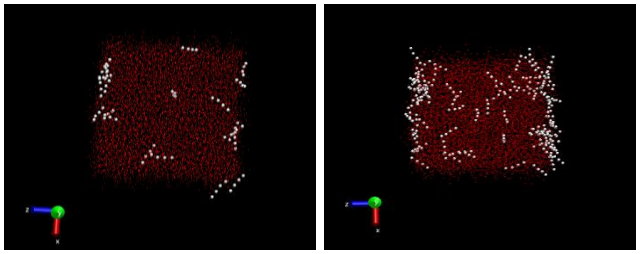

Figure 4 – Snapshots from MD simulation of $F_{12}H_{14}$ in H_{12} at 1%mol (left) and 4%mol (right). White spheres represent the fluorinated beads of the solute; red dots stand for the solvent beads.

The influence of temperature and concentration on ST was studied – since PFAAs have a surfactant effect in alkane solvents, it was confirmed that higher concentrations progressively contribute to lower the surface tension, an effect shared by higher temperatures - in part due to the entropic effect that reduces the extent of adsorption. The influence of these parameters is summarized in Fig. 5.

Subsequently, simulations of other PFAAs (F_3H_{23}, F_9H_{17}, $F_{21}H_5$, with the same 26 carbon atoms) were performed to investigate the influence of the fluorine content on the organization of PFAAs. At 1%mol, the four solutes are ranked according to their fluorine content – the more fluorinated the SFA, the higher the decrease in surface tension. This result is consistent with the fact that fluorocarbons have a generally lower surface tension than hydrocarbons, and so a more fluorinated SFA has a greater surfactant effect than a more hydrogenated one. Whilst the three bottom points are statistically equal, we believe that experimental data will prove that they rank, from top to bottom: F_9H_{17}, $F_{12}H_{14}$ and $F_{21}H_5$.

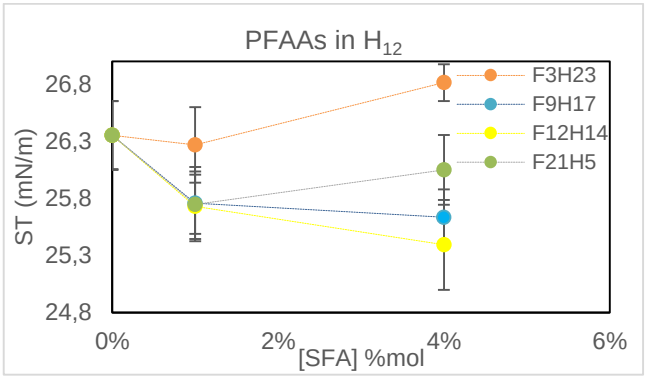

Figure 5 – ST of mixtures of PFAAs in H_{12} at 50ºC.

However, whilst the trend of stabilization of the surface advances for both $F_{12}H_{14}$ and F_9H_{17} (again, with the more fluorinated contributing more to reduce the ST), it actually inverts for F_3H_{23} and $F_{21}H_5$. For the latter, snapshots (see Fig. 7) suggest the formation of precipitates at the surface, which render the computation of ST a meaningless value. Thus, the increase cannot be isolated from the likely underwent solid-liquid transition. Regarding F_3H_{23}, our hypothesis (subject to experimental validation) is that its surfactant effect is so hampered that, at 4%mol, it has been outdone by the inevitable increase in ST that the addition of a longer alkane (and F_3H_{23} is an "almost-alkane") brings [23]. Because of this, it barely adsorbs (as Fig. 7 hints) and, at 4%mol, shows what could be some aggregates in the bulk.

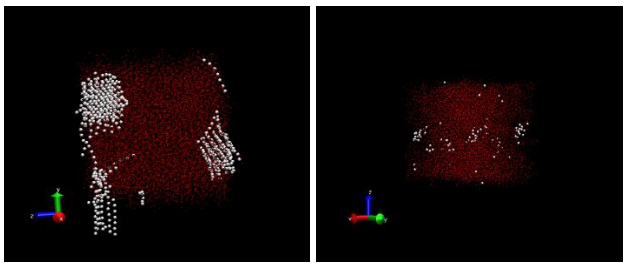

Figure 6 – Snapshots for $F_{21}H_5$ (left) and F_3H_{23} (right) at 4%mol. Red dots represent the solvent; white spheres stand for the fluorinated beads of the solute.

In a hydrocarbon solvent, PFAAs propensity to adsorb is intrinsically related with the length of the fluorinated chain. Longer chains not only promote more adsorption but also contribute, beyond the critical concentration, to the formation of aggregates. However, this ability to self-assembly depends heavily on the temperature (which, if below the Krafft Temperature, blocks the formation of aggregates on solubility grounds).

4.2.2 PFAAs in perfluoroheptane

Let one consider the new case of a PFAA solute in a fluorocarbon solvent. Because hydrocarbons have a higher surface tension than fluorocarbons, the adsorption of PFAAs is hindered, as it would destabilize the surface. The solute tends, then, to concentrated in the bulk and perhaps aggregate, with the hydrogenated tails oriented outwards. This absence of adsorption of PFAAs in fluorocarbons is indeed reported in [3, 4].

Similarly, four solvents were simulated in F_7: $F_{18}H_6$, $F_{12}H_{12}$, F_9H_{15} and F_3H_{21}, at concentrations of 5%mol and 10%mol (see Fig. 8). Clearly, the addition of PFAAs increases the ST – after all, even in the absence of adsorption, PFAAs will nevertheless spend some time (statistically speaking) near the surface. At 5%mol, the value for $F_{18}H_6$ is detached from the remaining three (which can be deemed statistically identical), that is, the more fluorinated solute imparted the smallest increase in surface tension. This result confirms the influence of the fluorine content on this property: because alkanes have a higher ST than perfluoroalkanes, a more hydrogenated SFA is related to a greater incentive to rise the ST. In hydrocarbon solvents, they bring a smaller reduction in this interfacial property; in fluorocarbon solvents, they promote a higher rise. Moreover, the overlapping of the remaining three points is considered unlikely, and one could expect that experimental results would rank them according to decreasing fluorine content.

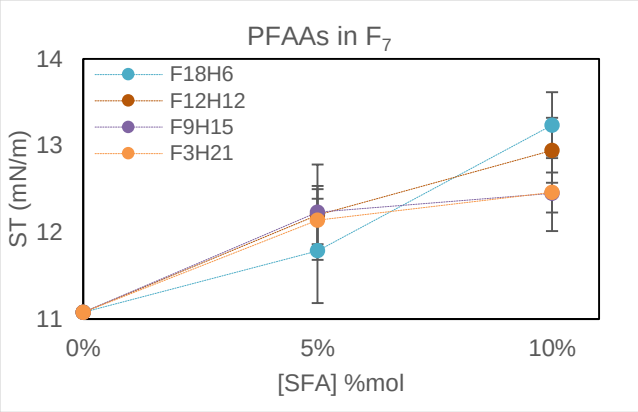

Figure 7 - ST of mixtures of PFAAs in F_7 at 45ºC.

At higher concentrations, an inversion is observed in the ranking of points (the most fluorinated solutes now promote the highest ST). This inversion may be rooted in aggregation. Longer alkane chains are associated with a larger driving force to aggregate. By forming aggregates in the bulk, PFAA molecules are less likely to move towards the surface, thus reducing the impact on the ST.

Fig. 8 shows that, at 5%mol, PFAAs tend to *negatively adsorb* in perfluoroheptane, moving away from the surface; for F_3H_{21} (on the right), in particular, some aggregation can be recognised, with some areas in the bulk more populated by the alkane chains than others.

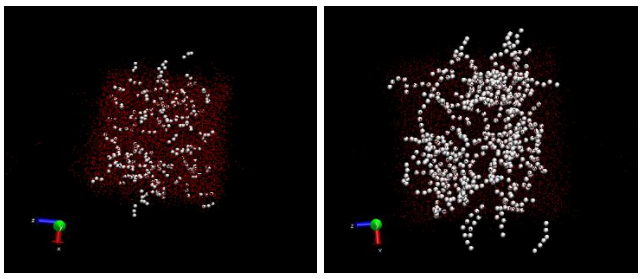

Figure 8 - Snapshots of F_9H_{15} (left) and F_3H_{21} (right) in F_7, at 5%mol and 45ºC. Red dots represent the solvent; white spheres stand for the hydrogenated beads of the PFAA molecules.

5. Conclusion

A heteronuclear force field of the SAFT-γ Mie family was refined with a rigorous description of intramolecular interactions and a more meaningful set of CG beads. The force field proved accurate in the prediction of bulk and interfacial properties. It also captured many subtleties of self-assembly arising from the addition of PFAAs to hydro- and fluorocarbon solvents, namely adsorption (positive and negative) as well as aggregation (likely through micellization). Future work will include experimental measurements of surface tension of the simulated mixtures.

6. References

1. Morgado, P., et al., *SAFT-γ force field for the simulation of molecular fluids: 8. Hetero-segmented coarse-grained models of perfluoroalkylalkanes assessed with new vapour–liquid interfacial tension data.* Molecular Physics, 2016. **114**(18): p. 2597-2614.
2. Broniatowski, M. and P. Dynarowicz-Łątka, *Semifluorinated alkanes—primitive surfactants of fascinating properties.* Advances in colloid and interface science, 2008. **138**(2): p. 63-83.
3. Binks, B., et al., *Semifluorinated alkanes as primitive surfactants in apolar hydrocarbon and fluorocarbon solvents.* Journal of molecular liquids, 1997. **72**(1-3): p. 177-190.
4. Binks, B., et al., *Adsorption and aggregation of semifluorinated alkanes in binary and ternary mixtures with hydrocarbon and fluorocarbon solvents.* Langmuir, 1997. **13**(25): p. 6669-6682.
5. Turberg, M.P. and J.E. Brady, *Semifluorinated hydrocarbons: primitive surfactant molecules.* Journal of the American Chemical Society, 1988. **110**(23): p. 7797-7801.
6. Marczuk, P., et al., *Gibbs films of semi-fluorinated alkanes at the surface of alkane solutions.* Langmuir, 2002. **18**(18): p. 6830-6838.
7. Nostro, P.L., et al., *Effect of a semifluorinated copolymer on the phase separation of a fluorocarbon/hydrocarbon mixture.* The Journal of Physical Chemistry, 1995. **99**(27): p. 10858-10864.
8. Watkins, E.K. and W.L. Jorgensen, *Perfluoroalkanes: Conformational analysis and liquid-state properties from ab initio and Monte Carlo calculations.* The Journal of Physical Chemistry A, 2001. **105**(16): p. 4118-4125.
9. Cui, S.T., et al., *Intermolecular potentials and vapor–liquid phase equilibria of perfluorinated alkanes.* Fluid Phase Equilibria, 1998. **146**(1): p. 51-61.
10. Potoff, J.J. and D.A. Bernard-Brunel, *Mie potentials for phase equilibria calculations: Application to alkanes and perfluoroalkanes.* The Journal of Physical Chemistry B, 2009. **113**(44): p. 14725-14731.
11. Voth, G.A., *Coarse-graining of condensed phase and biomolecular systems*. 2009, Boca Raton: CRC Press. xviii, 455 p., 16 p. of plates.
12. Papaioannou, V., et al., *Group contribution methodology based on the statistical associating fluid theory for heteronuclear molecules formed from Mie segments.* The Journal of chemical physics, 2014. **140**(5): p. 054107.
13. Noid, W., *Perspective: Coarse-grained models for biomolecular systems.* The Journal of chemical physics, 2013. **139**(9): p. 09B201_1.
14. Rahman, S., et al., *SAFT-γ force field for the simulation of molecular fluids. 5. Hetero-group coarse-grained models of linear alkanes and the importance of intra-molecular interactions.* (in press), 2014.
15. Song, W., P.J. Rossky, and M. Maroncelli, *Modeling alkane+ perfluoroalkane interactions using all-atom potentials: Failure of the usual combining rules.* The Journal of chemical physics, 2003. **119**(17): p. 9145-9162.
16. Duce, C., et al., *VLE and LLE of perfluoroalkane+ alkane mixtures.* Fluid Phase Equilibria, 2002. **199**(1): p. 197-212.
17. E. W. Lemmon, M.O.M., D. G. Friend. *Thermophysical Properties of Fluid Systems in NIST Chemistry WebBook, NIST Standard Reference Database Number 69 Eds. Linstrom, P.J.; Mallard, W.G.* . National Institute of Standards and Technology, Gaithersburg MD, 20899 [cited retrieved 2013; Available from: http://webbook.nist.gov.
18. Morgado, P., et al., *Liquid phase behavior of perfluoroalkylalkane surfactants.* The Journal of Physical Chemistry B, 2007. **111**(11): p. 2856-2863.
19. Morgado, P., et al., *Systems involving hydrogenated and fluorinated chains: volumetric properties of perfluoroalkanes and perfluoroalkylalkane surfactants.* The Journal of Physical Chemistry B, 2011. **115**(50): p. 15013-15023.
20. Müller, E.A. and G. Jackson, *Force-Field Parameters from the SAFT-γ Equation of State for Use in Coarse-Grained Molecular Simulations.* Annual Review of Chemical and Biomolecular Engineering, 2014. **5**(1): p. 405-427.
21. Vandana, V., D.J. Rosenthal, and A.S. Teja, *The critical properties of perfluoro n-alkanes.* Fluid phase equilibria, 1994. **99**: p. 209-218.
22. Matsuda, H., et al., *Liquid–liquid equilibrium data for binary perfluoroalkane (C 6 and C 8)+ n-alkane systems.* Fluid Phase Equilibria, 2010. **297**(2): p. 187-191.
23. Rolo, L.I., et al., *Surface tension of heptane, decane, hexadecane, eicosane, and some of their binary mixtures.* Journal of Chemical & Engineering Data, 2002. **47**(6): p. 1442-1445.